

ZIRCONIUM IRON DISPROPORTIONATION DURING HYDRIDING REACTIONS IN NUCLEAR GETTERING OPERATIONS

Michael Coleman¹, Dhanesh Chandra¹, Joseph Wermer², and Terrence J. Udovic³

¹Materials Science and Engineering
MS 388 University of Nevada Reno; 1664 N. Virginia St.; Reno, NV 89557

²Los Alamos National Laboratory
P.O. Box 1663, Los Alamos, NM 87545

³NIST Center for Neutron Research
100 Bureau Drive, MS 8562, Gaithersburg, MD 20899

Keywords: zirconium-iron hydride, disproportionation, inelastic neutron scattering

Abstract

We have investigated the hydriding properties of Zr_2Fe and Zr_3Fe alloys, including SAES Getters St-198. It was found from examining the X-ray diffraction patterns of alloys hydrided at temperatures ranging from 303 K to 773 K that disproportionation occurs in the Zr_2Fe alloys at temperatures above 673 K. In Zr_3Fe the temperature at which disproportionation takes place is much lower being between 473 and 573 K. In order to study the thermodynamics of hydride formation for these alloys pressure composition isotherms were recorded at temperatures between 303 and 773 K. Similarities in the x-ray diffraction patterns of partially hydrided Zr_2Fe and Zr_3Fe samples has prompted the use of inelastic neutron scattering to characterize the hydride products formed.

I. Introduction

In nuclear processing plants the formation and release of tritiated heavy waters to the environment is a serious concern [1, 2]. At Los Alamos National Laboratory (LANL) processing facility, tritiated waters are first cracked to obtain gaseous tritium, which is then mixed with a nitrogen carrier gas. The tritium nitrogen mixture is passed through a heated bed of the SAES Getters St198. The getter, St198, nominally Zr_2Fe , was chosen to scavenge trace amounts of tritium in nitrogen streams. The getter can absorb tritium at low absorption pressure, combined with low reactivity with the carrier nitrogen gas at moderate temperatures. Bench scale testing of these getters (5-15 grams of St 198 pellets) was performed using deuterium gas at 523 K to saturation and unloaded at 973 K under vacuum. The pellets remained effective for approximately 10 cycles before serious loss of capacity that required getter-pellet replacement. Understanding of the phase equilibria during hydriding and dehydriding reactions is necessary to increase the longevity of this material.

The existing phase diagrams [3-6] were examined to compare for thermodynamic consistency. Havinga et al. [5] reported a Zr-Fe phase diagram with a stable Zr_2Fe phase at room temperature; stable up to 1220 K. More recent phase diagrams by Arias [6], and Okamoto [3] show Zr_2Fe as a high temperature phase in equilibrium between 1048 K and 1123 K. More recently, Servant et al. [4] reported a calculated Zr-Fe phase diagram using thermodynamic functions. In this phase diagram Zr_2Fe and Zr_3Fe are shown as equilibrium phases at 500K. The Zr-Fe system was investigated by Aubertin et al. and Zr_2Fe was determined to be a high temperature phase [7]. The dehydriding temperature used by LANL in their bench scale experiments is high enough that equilibration of a metastable phase is possible, and therefore hydriding characteristics of both Zr_2Fe and Zr_3Fe are necessary. Thus, structural and thermodynamic studies were needed on the Zr-Fe system.

Thermodynamic and structural properties of Zr_2Fe and Zr_3Fe intermetallics have been studied by several investigators. Havinga [5] determined the structure of Zr_2Fe as body centered tetragonal (space group, $I4/mcm$) by x-ray diffraction methods. Yartys et al [8-10] confirmed this crystal structure by using neutron diffraction methods. Dey and Banerjee [11] determined the structure of Zr_3Fe to be orthorhombic ($Cmcm$) by x-ray diffraction method. Yartys et al. [8-10] also confirmed this Zr_3Fe structure by using neutron diffraction. Boffito et al. [1] and Nobile et al. [2] reported compositional details of the phases by characterizing polished sections in an electron microprobe study. In Boffito's [1] study, they reported composition of 76.5% Zr and 23.5%Fe that suggests that Zr_2Fe in St 198 is stable at room temperature; he also reported presence of α -Zr and minor quantities of other unidentified phases. Nobile et al. [2] performed a very detailed study and found Zr_2Fe , $ZrFe_2$, α -Zr, Zr_6Fe_3O , and a minor phase of Zr_5FeSn , in St198. Nobile et al. [2] also hydrided St198 in a temperature range of 473 and 773 K. Aubertin et al. hydrided Zr_3Fe at different concentrations and reported the x-ray diffraction results. In the course of experimentation it was noted that the Zr_3Fe hydride was subject to disproportionation to ZrH_2 and $ZrFe_2$ at temperatures above 770 K [21]. Yartys et al. [7, 9] made single phase Zr_2Fe as well as Zr_3Fe intermetallic phases. Hydriding of these phases were performed at room temperature, while monitoring the amount of hydrogen introduced in the crystal. The crystal structures of Zr_2Fe and Zr_3Fe deuterides were determined using neutron powder diffraction methods. The structure of Zr_2FeD_5 was determined as primitive tetragonal ($P4/ncc$), while the $Zr_3FeD_{6.7}$ was orthorhombic ($Cmcm$) [3].

II. Experimental Methods

II.1 Sievert's Apparatus

Hydrogen adsorption isotherms were obtained using an automated University of Nevada Reno's Sievert's apparatus. Our manifold is a cylinder with 10 ports equally spaced radiating off of the center and an eleventh port leaving axially from the back panel. Two pressure transducers were used; one a 10,000 Torr DataMetric, and the other a 1 Torr MKS Baratron pressure transducer. Temperature was monitored at the sample holder, and at the manifold using K-type thermocouples. Vacuum was obtained by a Varian V70 turbo system pump with a dry backing pump. All of the volumes in the apparatus have been carefully measured by either directly using acetone or by calculation from other known volumes. Sample temperature was controlled outside the Sievert's control program using a Watlow surround heater and a Love Controls PID controller. The sample was placed in a stainless steel holder attached to the lowest port.

Activation is necessary to initiate zirconium iron hydride formation. Yartys et al. [7, 9] used chemical cleaning followed mechanical cleaning to activate samples effectively. Nobile et al. [2] heated the samples in vacuum to at least 623 K for 4 to 16 hours. In this study vacuum was applied to the sample taking the pressure down to <0.1 mtorr. To ensure activation the samples were heated to 553 K for one hour in vacuum. These Zr_3Fe and Zr_2Fe button samples were made at LANL by arc melting stoichiometric amounts of zirconium and iron in an argon atmosphere. The Zr_3Fe buttons were then annealed for 60 hours at 933 K. Upon completion of a hydride formation isotherm collection the intermetallic was immediately subjected to a desorption isotherm that incrementally removed the hydrogen from the apparatus. Subsequently, the sample temperature was reduced to room temperature after which the sample was removed from the Sievert's apparatus.

II.2 X-Ray Diffraction Studies

In ex-situ x-ray diffraction studies on hydrided Zr-Fe intermetallics were performed under atmospheric conditions. In some cases, grinding of pyrophoric samples triggered rapid oxidation that resulted in oxidization of the entire sample; grinding was therefore kept to a minimum in all cases. The powders were placed on a quartz slide and the x-ray diffraction

patterns were obtained using diffractometers equipped with the MDI DataScan software. X-ray diffraction patterns were obtained on one of two Phillips θ -2 θ Bragg-Brentano Diffractometer using copper K-alpha radiation. The power settings varied depending on the equipment used and were 35 kV and 25 mA for our diffractometer and 40 kV and 40 mA while using the Nevada Bureau of Mines, University of Nevada, Reno diffractometer.

II.3 Inelastic Neutron Scattering Experiments on Zr_2Fe and Zr_3Fe

Using the NIST Center for Neutron Research (NCNR) Seivert's apparatus samples of Zr_2Fe (St198 and LANL prepared button) and Zr_3Fe (LANL prepared button) were deuterated. The intermetallics were placed in a quartz tube and evacuated. The temperature was raised to 573 K and the sample was allowed to degas for one hour. The metal samples were then cooled to room temperature and deuterated as per above, resulting in fully deuterated room temperature Zr_2Fe (St198 and LANL button) and Zr_3Fe (LANL button) samples. Each sample was then loaded separately into vanadium canisters, while in a helium glove box. Samples were cooled to 10 K using a cryostat, which was in place during the experiment. The neutron energy was then scanned from 30 to 200 meV.

III. Results

III.1 Hydriding characteristics of Zr_2Fe and Zr_3Fe .

The pressure composition isotherms for Zr_2Fe demonstrate an increase in plateau pressure which accompanies with the increase in temperature. The shapes of the isotherms are similar for temperatures up to 773 K, at which a significant change in pressure may be noted at a H/M value of approximately 0.35, as seen in Figure 1. X-ray diffraction results from the isotherm

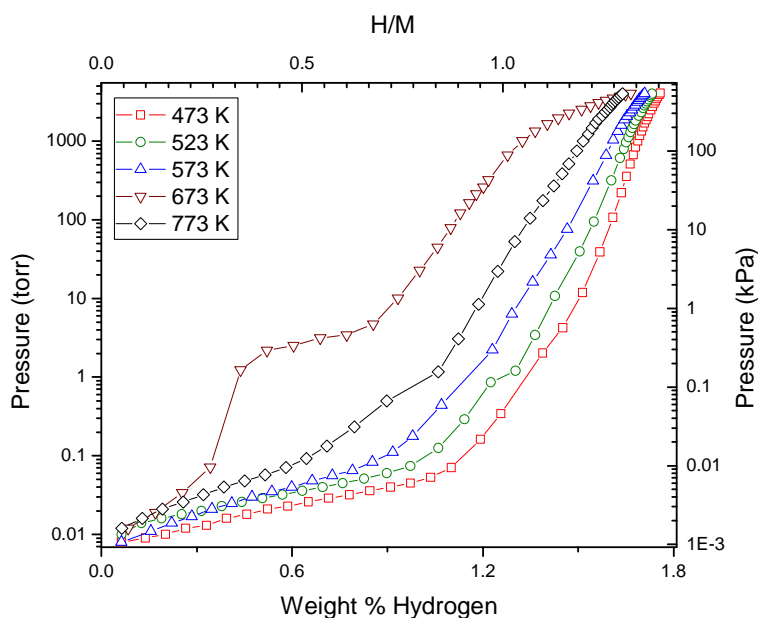


Figure 1. High temperature Pressure Composition Isotherm for Zr_2Fe (St198).

products reveal that the hydride formed at 473 K as shown in the isotherm match well with the JCPDS file 41-1066 for $Zr_3FeH_{5.6}$. As the temperature is increased the hydride products no longer match this pattern but there are still similarities in the profile. Fitting the x-ray diffraction pattern to published structures of zirconium-iron hydrides, has resulted in a best fit which matches the tetragonal P4/ncc structure used by Yartys et al. for Zr_2FeH_x . Figure 2 demonstrates that this structure matches the lower temperature products, with peak shifts accompanying the lower degree of loading at elevated temperatures. However when the products of the 723K isotherm were examined, it was found that disproportionation had

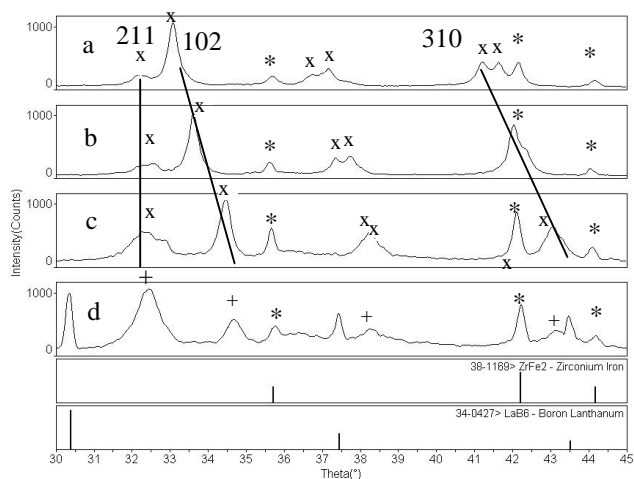


Figure 2. X-ray diffraction patterns of products from Zr_2Fe hydriding experiments. (a) 473 K, (b) 573 K, (c) 673 K, (d) 723 K. * $ZrFe_2$, + ZrH_2 , x Zr_2FeH_x .

occurred and ZrH_x was formed. This change in structure coincides with the change in shape of the isotherm that was found.

Isotherms for the Zr_3Fe intermetallics are shown in Figure 3. The plateau observed for the 373 K isotherm appears at a higher pressure than that of 473 and 573 K isotherms, which is inconsistent with the temperature change in the *low pressure plateau region*. The x-ray diffraction results confirm a Zr_3FeH_x phase formed at 373 and 473 K, from the isotherm experiment reaction products. However, the products produced at and above 573 K show disproportionation with formation of ZrH_x . In addition, the Bragg peak widths for the 773 K diffraction pattern are much smaller than those for peaks observed in 573 and 673 K patterns.

At low temperatures (up to 673 K) the Bragg peak width of the disproportionated phase, ZrH_x , were wide, suggesting micro-strains, $\langle \epsilon^2 \rangle^{1/2}$, were present in the lattice of this phase. As the

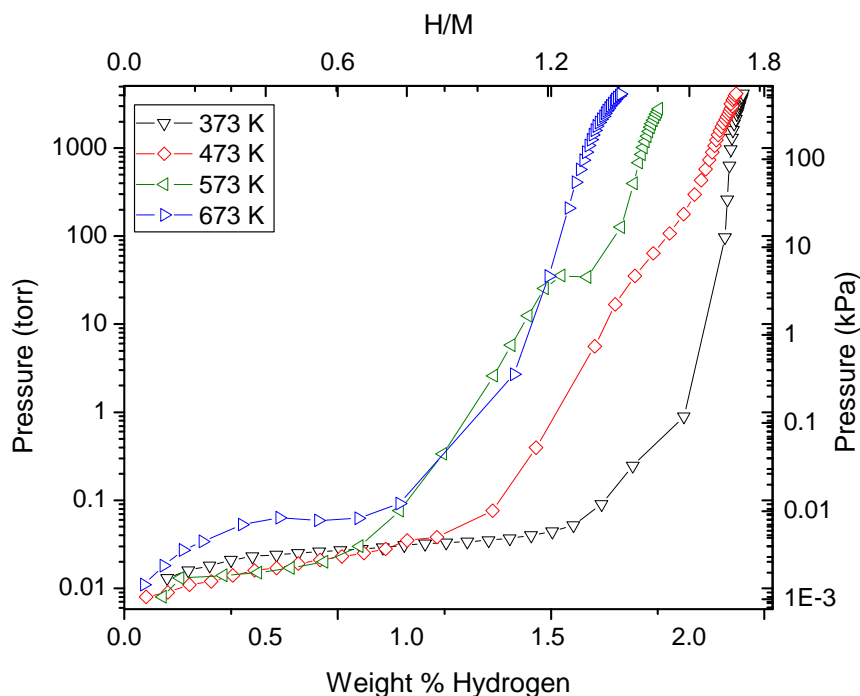


Figure 3. Pressure composition Isotherms of Zr_3Fe in hydrogen for temperatures of 373 to 673 K.

temperature was increased, above 673K), further disproportionation occurred yielding α -Fe phase and ZrH_2 . It should be noted that the Bragg peaks widths of ZrH_2 reduced significantly suggesting that the α -Fe phase precipitation released the micro-strain in the structure of ZrH_2 .

III.2 Inelastic Neutron Scattering of Zr_2Fe and Zr_3Fe Hydrides and Deuterides

We had difficulties in determining the hydride phases present in the zirconium-iron hydride due to structural changes of the parent phase during heating and hydriding. We performed inelastic

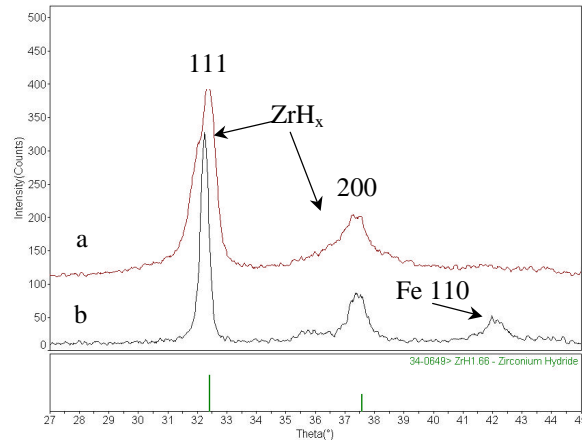


Figure 4. X-ray diffraction pattern of Zr_3Fe after disproportionation. (a)673K (b) 773K

neutron scattering to offer possible characterization alternatives to x-ray diffraction methods. Vibrational inelastic neutron scattering patterns of Zr_2Fe and Zr_3Fe deuterides made at 303K, and hydrides made at 723K are shown in Figure 5. It should be noted that the patterns for hydrides made at 723K show a partially and fully hydrided Zr_2Fe . For comparison purposes the hydride patterns have been shifted by dividing the energy by the square root of two, in order to account for mass differences between the hydrogen atom and the deuterium atom. The low temperature deuterides of Zr_2Fe and Zr_3Fe have well defined differences in both energy and shape that are adequate for determining deuteride phases. More importantly the patterns for the Zr_2FeD_x (Zr_2Fe alloy made in house) button and commercial St198, are quite similar despite the impurity phases that are present in the commercial product. Examination of the graphs of the high temperature partially and fully hydrided Zr_2Fe has provided further information with regards to the vibrational patterns of zirconium hydrides. Although only an approximation of

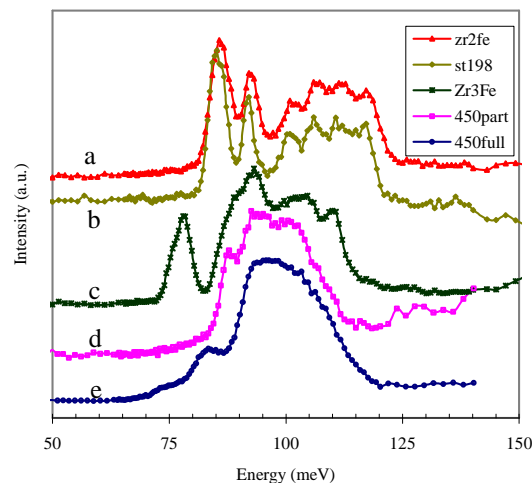


Figure 5. Inelastic Neutron Scattering Patterns for Zr_2Fe and Zr_3Fe deuterides and hydrides. From top to bottom (a) Zr_2Fe (button) deuteride, (b) Zr_2Fe (St198) deuteride, (c) Zr_3Fe (button) deuteride, (d) Zr_2Fe (St-198) partial hydride formed at 723K, (e) Zr_2Fe (St-198) hydride fully loaded at 723K.

the energies and shape of a zirconium deuteride this graph does show that we can distinguish between all three hydride or deuteride phases shown.

IV. Discussions

In order to increase the lifetime of gettering materials in the nuclear industry the hydride products of Zr_2Fe and Zr_3Fe at several temperatures have been compared. It was found that Zr_2Fe demonstrates an elevated hydride stability over that of Zr_3Fe . From these experiments the Zr_3Fe was found to disproportionate into ZrH_x at temperatures between 473 and 573 K. Zr_2Fe on the other hand was able to produce stable hydrides up to 673 K. The operating temperature of the gettering bed in the Los Alamos experiments is 523 K which falls in the temperature range that might result in formation of ZrH_x depending on the phases present in the getter bed. The metastable nature of Zr_2Fe below 1048 K has raised questions as to the hydride products that are being formed. We have shown that these products match the JCPDS file 41-1066 for $Zr_3FeH_{5,6}$, which we initially interpreted as hydrogen migration through the crystal allowing equilibration of the metastable Zr_2Fe phase to Zr_3Fe and $ZrFe_2$. However the match obtained between the diffraction patterns of the 473 to 673 K hydride products and the structural data for Zr_2FeH_x support the assertion that in this case Zr_2FeH_x is the phase being formed.

The increased robustness of the Zr_2Fe against disproportionation becomes important when the method of recycling is examined. For the Los Alamos National Laboratory gettering system the getter is heated to 973 K in vacuum. This temperature is great enough to proceed with the transformation to the equilibrium composition of Zr_3Fe and $ZrFe_2$. Operation of the gettering beds at 523 K could ultimately result in the disproportionation of the Zr_3Fe that is formed during the dehydriding portion of the cycle. The hydrogenation-disproportionation-desorption-recombination (HDDR) cycle that was proposed by Yartys et al [9] would only be possible if the dehydriding temperature of the getter bed was increased to at least 1048 K, which according to the phase diagram of Okamoto [3] is the lower limit of the Zr_2Fe equilibrium phase. As this elevated temperature might be prohibitive in the current system, reducing the bed temperature to 473 K should increase the lifetime of the getter.

VII. Conclusion

In this study we have shown that Zr_2Fe hydrides have elevated thermal stability when compared to Zr_3Fe hydrides. Alternatives are given to increase the lifetime of the SAES getter St198 in tritium gettering applications. Inelastic neutron scattering data has been used to demonstrate the ability to characterize zirconium-iron hydrides and deuterides. Future inelastic neutron scattering work will deal with modeling the interactions of the hydrogen species in the zirconium-iron lattice.

VIII. Acknowledgement

We would like to express our appreciation for the support from Los Alamos National Laboratory in the funding of this research. Also our thanks to Dr. Terrence J. Udovic for help in the use of the NIST Center for Neutron Research facilities.

IX. References

- 1 Boffito C., Doni F., Rosai L., *Journal of the Less Common Metals*, 104 (1984) 149.
- 2 Nobile A., Mosley W.C., Holder J.S., Brooks K.N., *Journal of Alloys and Compounds*, 206(1994)83.
- 3 Okamoto H., *Journal of Phase Equilibrium*, 14(5) (1993) 652.
- 4 Servant C., Gueneau C., Ansara I., *Journal of Alloys and Compounds*, 220 (1995) 19.

- 5 Havinga et al, *Journal of Less Common Metals*, 27 (1972) 169.
- 6 Arias D., J.C. Abriata, in Massalski et al. (Ed.), *2nd ed, Binary Alloys Phase Diagrams, Vol. 2, ASM International, USA*, (1990) 1798.
- 7 Aubertin F., Gonser U., Campbell S., Wagner H. *Z. Metallkde.* 76 (1985) 237.
- 8 Yatrýs V.A., Fjellvag H., Hauback B.C., Riabov A.B., *Journal of Alloys and Compounds*, 274 (1998) 217.
- 9 Yatrýs V.A., Fjellvag H., Harris I.R., Hauback B.C., Riabov A.B., Sorby M.H., Zavalíy I., *Journal of Alloys and Compounds*, 293-295 (1999) 74-87.
- 10 Yatrýs V.A., Fjellvag H., Harris I.R., Hauback B.C., Riabov A.B., Sorby M.H., Zavalíy I., *Journal of Alloys and Compounds*, 265 (1998) 6-14.
- 11 Dey G., Banerjee S., *Material Science Engineering*, 73 (1985) 187.
- 12 Aubertin F., Whittle G., Campbell S., Gonser U., *Phys. Stat. Sol. (a)* 104 (1987) 397.
- 13 for GSAS, *J. Appl. Cryst.* **34**, 210-213 (2001).
- 14 A.C. Larson and R.B. Von Dreele, "General Structure Analysis System (GSAS)", Los Alamos National Laboratory Report LAUR 86-748 (2000).
- 15 JCPDS files